Production Strategy for Manufacturing Large-Scale AlSi10Mg Components by Laser Powder Bed Fusion

FEDERICO BOSIO,[1,2,3] HAOPENG SHEN,[1,2] YANG LIU,[1,2]
MARIANGELA LOMBARDI,[3] PAUL ROMETSCH,[1,2,4] XINHUA WU,[1,2]
YUMAN ZHU [1,2,5] and AIJUN HUANG[1,2,6]

1.—Monash Centre for Additive Manufacturing, Notting Hill, VIC 3168, Australia. 2.—Department of Materials Science and Engineering, Monash University, Clayton, VIC 3800, Australia. 3.—Department of Applied Science and Technology, Politecnico di Torino, Corso Duca degli Abruzzi 24, 10129 Turin, Italy. 4.—*Present address:* Arvida Research and Development Centre, Rio Tinto, Jonquiere, QC G7S 4K8, Canada. 5.—e-mail: yuman.zhu@monash.edu. 6.—e-mail: aijun.huang@monash.edu

The long production time required for large-scale parts fabricated by laser powder bed fusion (LPBF) tends to induce cracks, distortions, and overheating problems. In this work, to address these challenges, we explored and established a suitable strategy for producing large AlSi10Mg components. The platform temperatures to prevent cracks and distortions were firstly determined. Then, the in situ aging behavior was investigated for samples under various platform temperatures and holding times. Our results revealed that platform temperatures of 150°C and 200°C can effectively prevent cracks and minimize distortions. Besides, using 150°C, samples can reach peak hardness with a holding time less than 13 h. In comparison, those samples produced with a holding time longer than 13 h at 150°C and 200°C show obvious over-aging responses and thus lower hardness. However, such a hardness impoverishment can be recovered by using a T6 post-process heat-treatment.

INTRODUCTION

Laser powder bed fusion (LPBF), as one of the typical additive manufacturing (AM) technologies, is a profitable alternative to conventional casting for the production of complex-shaped metal parts.[1,2] However, former LPBF printing machines with limited building chamber dimensions only allow the fabrication of small-sized components. Therefore, LPBF systems with higher building volumes have been introduced to the market for large-scale manufacturing. Nevertheless, producing massive components made of aluminum alloys by LPBF still involves essential challenges to tackle. One issue is represented by the internal residual stresses arising from the rapid solidification. Such stresses will generate severe distortion and cracks, and will eventually lead to job failure.[3] Since the LPBF

Federico Bosio and Haopeng Shen contribute equally to the work.

process is relatively slow compared with foundry techniques, building large parts by LPBF requires rather a long printing time. Consequently, those defects must be prevented to save time and powder. On this basis, heating the building platform throughout printing has been suggested to be effective in alleviating residual stresses and deformation of built parts.[4] Also, the heated building plate can reduce the solidification shrinkage of components due to the reduced thermal gradient.[4,5]

Over the last decade, the Al-Si based alloys, i.e., 4xxx aluminum alloys, have been widely processed by LPBF because their final products potentially meet the industrial requirements in terms of being lightweight, having shape freedom, and good thermal conductivity.[6–10] Since these alloys can be age-hardened,[11] the platform heating strategy can also induce the age-hardening effects to further improve the mechanical properties of the products, besides alleviating distortions and cracks.[12–14] Specifically, Aversa et al. investigated the effect of various building platform temperatures on the

strength and microstructure of an LPBF-produced A357 alloy.[12] Their results revealed the appearance of Mg_2Si precipitates at different building platform temperatures due to the in situ aging induced by the heated platform during LPBF. Later, similar precipitates were confirmed by using differential scanning calorimetry (DSC) to examine the thermal ramp of an AlSi10Mg alloy processed by selective laser melting (SLM) with a platform heated to 160°C.[13] However, the hardness profile of a cylindrical bar of 100 mm in length did not show any significant age-hardening response along the building direction.[13] Recently, the precipitation of Si particles at a nano-scale has been reported in the as-built SLM-produced A357 alloy with a platform temperature of 80°C.[14] Also, satisfactory tensile properties were reported, although the alloy exhibited a relatively low hardness in both as-built and directly aged conditions. The reason was mainly ascribed to the loss of solid-solution strengthening caused by the formation of nano-precipitates. Buchbinder et al. performed a systematic investigation on the effect of varied platform heating temperatures on distortions of AlSi10Mg components processed by SLM.[15] It was concluded that a platform temperature of 250°C was appropriate to completely prevent distortions, although a low hardness value ($\sim$ 80 HV) was associated with the material. This value, however, is still higher than the hardness standard DIN EN 1706 for die-cast counterparts. Nonetheless, for the production of large-scale components, this hardness impoverishment could be further encouraged by the long holding time above the heated platform and, therefore, more research is needed to solve this issue.

In this work, a production strategy for manufacturing large parts made of AlSi10Mg by LPBF is proposed. Two main vital design aspects are concurrently addressed for the first time. The first is the prevention of cracks and support distortions, which may lead to job failure. By using the platform heating strategy, we first determined the platform temperatures that can alleviate macro-residual stresses by using an optimized processing setup. Then, the second crucial aspect addressed in this work is the age-hardening effect induced by the heated platform. In this aspect, by producing the same samples with different printing times on a platform heated at 150°C, we clearly show that the in situ aging behavior not only depends on the holding time on the heated platform but also the position along the building direction. Also, the printing time limit to avoid in situ over-aging at 150°C was determined. Finally, for the production of large-scale parts with a platform temperature of 200°C, it was demonstrated that over-aging occurs during printing, and a post-process heat treatment can effectively increase the hardness.

MATERIALS AND METHODS

Powder and LPBF Process

Pre-alloyed gas-atomized powder of AlSi10Mg (TLS Technik GmbH & Co., Bitterfeld) was used in this work. The chemical composition of the powder can be found in supplementary Table S-I. Direct current emission spectroscopy was used to detect metal elements (ASTM E 1097-12), while oxygen and nitrogen were analyzed via inert gas fusion (ASTM E 1019-11). The field-emission gun scanning electron microscope (SEM) JEOL JSM-7001F was used to evaluate particle shape and morphology. The size distribution was determined using laser diffraction analysis (Malvern Mastersizer 2000). Most particles of the gas-atomized powder have a spherical shape (Fig. 1a), and a mean size of 34 μm (Fig. 1b).

The optimized processing parameters in an EOS M290 system (EOS Gmbh) have been adopted in this work to manufacture the AlSi10Mg specimens, see supplementary Table S-II. A Yb-fiber laser with a wavelength of 1060–1100 nm and a nominal power of 370 W were used to melt a thin powder layer locally. The scanning speed of the laser was 1300 mm/s. Also, argon gas was applied in the building chamber to reduce the oxygen content below 0.1%. In addition, a 67° rotated scanning strategy was adopted to achieve isotropic properties in the plane parallel to the building platform.[16] A heated building platform was utilized to investigate its effects on the cracks, distortions, and the in situ aging response. It is worth noting that this strategy is different from platform preheating for LPBF.[17,18] We kept the platform at a constant temperature (T) throughout the building process. The specific T levels used in this study were selected based on previous work, see supplementary Table S-II.[7,12–14]

Cracks and Distortions Assessment

The production of large parts can prematurely fail during LPBF when the internal residual stresses lead to severe distortions, cracks, delamination, and buckling. In this work, the platform heating method was applied to alleviate these phenomena. To study the effect of various building platform temperatures on the formation of cracks and distortions, the 'twin cantilever' method proposed by Buchbinder et al.[15] was adopted for this work. Cantilever samples with twin arms of 50 mm in length and 3 mm in thickness (Fig. 2) were built at T of 45°C room temperature (RT), 100°C, 150°C, and 200°C. Surface profiles were recorded using a Mitutoyo CRYSTA-Apex S700 CNC coordinate measuring machine with a position accuracy of 1.7 μm to obtain the reference baseline. Then, support fins of the right-hand arm were cut using electric discharging machining in the proximity of the building plate. All cantilever profiles were measured again to evaluate the extent of arm deflection after removal
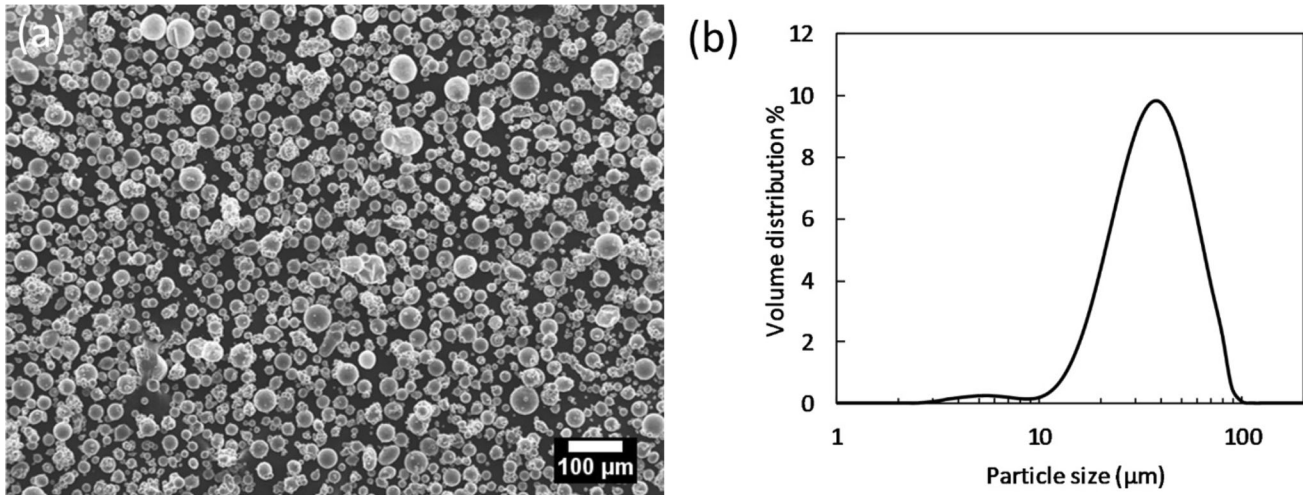
Fig. 1. (a) AlSi10Mg powder observed by SEM, and (b) powder size distribution.

from the building plate. Profile measurements were carried out along the middle axis of the cantilever with a probe displacement of 1 mm. Five cantilever profiles for each condition were averaged to determine the overall deflection curve. On this basis, the appropriate platform heating temperatures were selected for the further in situ aging study.

In-Situ Aging Assessment

Building large parts by LPBF may require a long printing time (up to 1 week occasionally). The LPBF printing time, t, relies on the process parameters and volume number of parts to be printed. For this reason, two AlSi10Mg jobs with a low and high packing density of samples, corresponding to a LPBF printing time t of 13.4 h and 53 h respectively, were designed (Fig. 3). Parallelepiped samples with dimensions of $11 \times 85 \times 35$ mm^3 were built by using a platform heating at 150°C. The Vickers micro-hardness (HV0.5) was evaluated along the building direction of as-built samples using the Duramin A330 hardness tester with a load of 0.5 kg and a dwell time of 10 s. Six samples for each condition were investigated to obtain the overall HV behavior. The hardness measurement was performed at specific height levels along the z-axis. A total of 30 measures was made for each height level. The LPBF holding time of each height level can be determined by

$$\tau_i = \frac{(h - h_{i\_HV})}{h} \cdot t \qquad (1)$$

where τ_i is the LPBF holding time corresponding to the specific hardness tested level h_{i_HV}, h is the total sample height (35 mm), and t is the LPBF printing time.

Samples for SEM investigation were ground and polished, and then etched in Kroll's reagent for 15 s. SEM images and energy-dispersive X-ray

spectroscopy (EDS) maps were obtained using the JEOL JSM-7001F microscope.

Post-Process Heat Treatments

Cubes with dimensions of $10 \times 10 \times 10$ mm^3 were produced using a platform heating temperature of 200°C and a printing time of roughly 10 h. To mimic the heated platform effect for large parts, we conducted a long-term isothermal heat treatment at 200°C for up to 100 h on the as-built samples. The temperature inside the furnace chamber was set at the same T used throughout LPBF and monitored by a thermocouple $(\Delta T \pm 1°C)$. Later, all samples were heat-treated by a T6-like solution (520°C/1 h + water quenching + 160°C/6 h) to evaluate the effect of such heat treatment on the hardness and microstructure. The gap time between solid solution and artificial aging was controlled and kept below 30 min. For each sample, five Vickers hardness (HV 0.5 kg/10 s) measurements along the building direction were performed according to ASTM E92-17.

RESULTS

By using the platform heating strategy, the platform temperatures able to prevent cracks were first examined to uncover a safe route for the production of large-scale components (Fig. 4a and b). The micrographs in Fig. 4a depict cantilever parts built at different platform heating temperatures T ahead of supports removal. A qualitative analysis of Fig. 4a reveals that various defects, such as cracks and support distortions, appear at 45°C and 100°C. The origin of these defects is associated with the first consolidated layers between the support structure and horizontal arms of twin cantilever samples. These distortions and cracks reduce significantly on the cantilevers built at 150°C and 200°C. The number of cantilever deflections as a function of the platform temperatures is
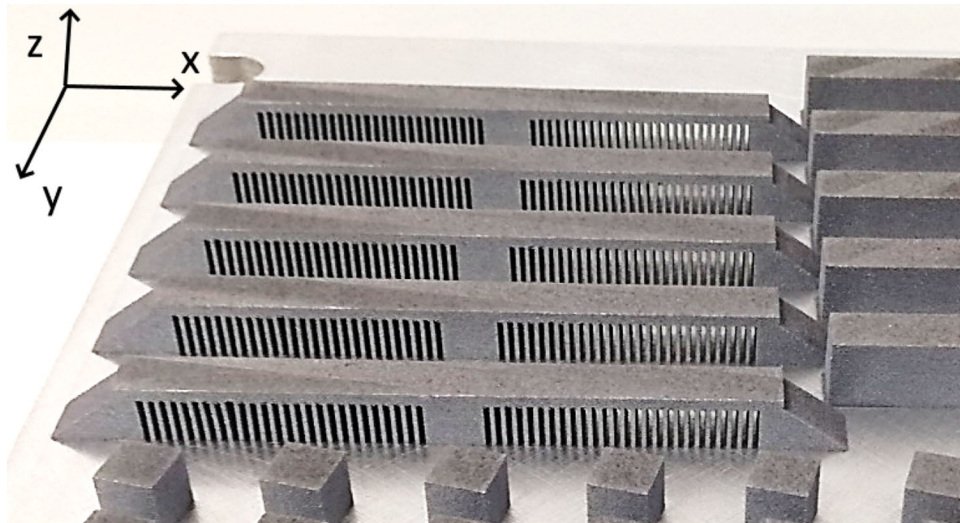
Fig. 2. Twin cantilever samples of AlSi10Mg alloy produced by LPBF. The *z*-direction represents the building direction.
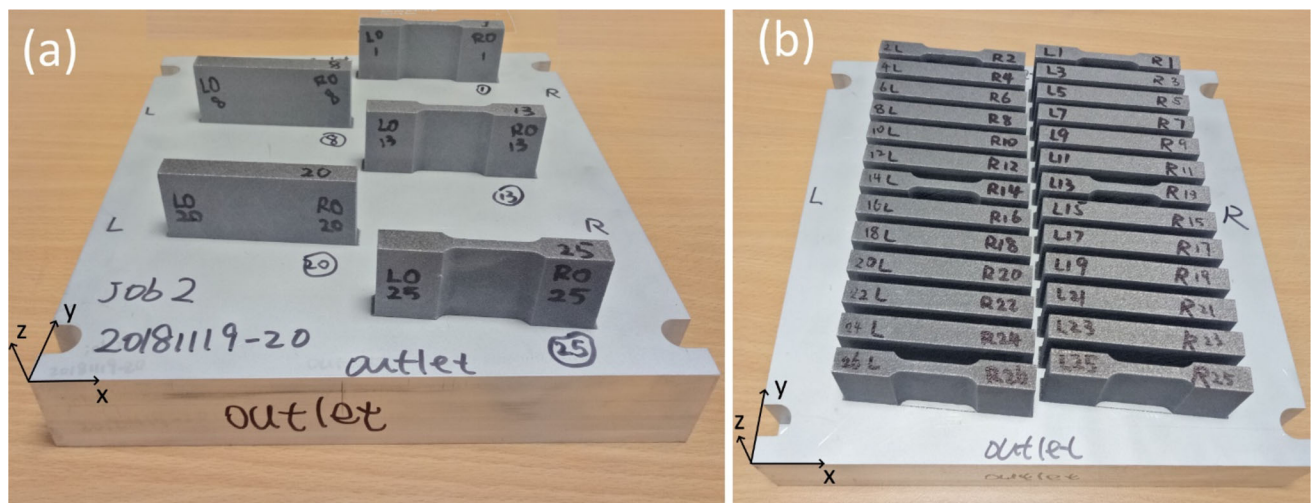

Fig. 3. (a) Low and (b) high packing density jobs of AlSi10Mg samples, corresponding to a total LPBF printing time of 13.4 h and 53 h, respectively. The z-direction represents the building direction.

shown in Fig. 4b. Given that most of the residual stresses generated in LPBF are released after support removal, they will give rise to the bent deflections associated with the samples. The maximum deflection ΔZ is recorded at the connection edge between the substrate and the cantilever built at 45°C. At higher platform temperatures, the ΔZ reduction measured at the cantilever edge was 34% and 54% for 100°C and 150°C, respectively. There was no obvious deflection detected at a platform temperature of 200°C.

Based on the results in Fig. 4a and b, both platform temperatures at 150°C and 200°C can effectively prevent crack formation and minimize distortions in cantilever parts, which is a vital requirement for a successful job when large LPBF parts are produced. Therefore, these two temperatures were selected for the subsequent in situ aging studies. It should be noted that the former melted i-layer close to the heated substrate experiences a longer holding time than the later consolidated one ($i + 1$ layer) during the LPBF process. Hence, the hardness associated with different sample height is likewise different. Figure 5 provides the hardness values along the z-direction of the samples of 35 mm in height that were built at a platform temperature of 150°C for 13.4 h and 53 h. Considering the hardness profile after a printing time of 13.4 h, there was a significant hardness increment when the building time reached 2.5 h, which corresponds with the top part of the sample (i.e., h is between 23.7 and 35 mm). Then the hardness reaches a plateau value of $\sim$ 137 HV between 2.5 h and 12.4 h. However, for the
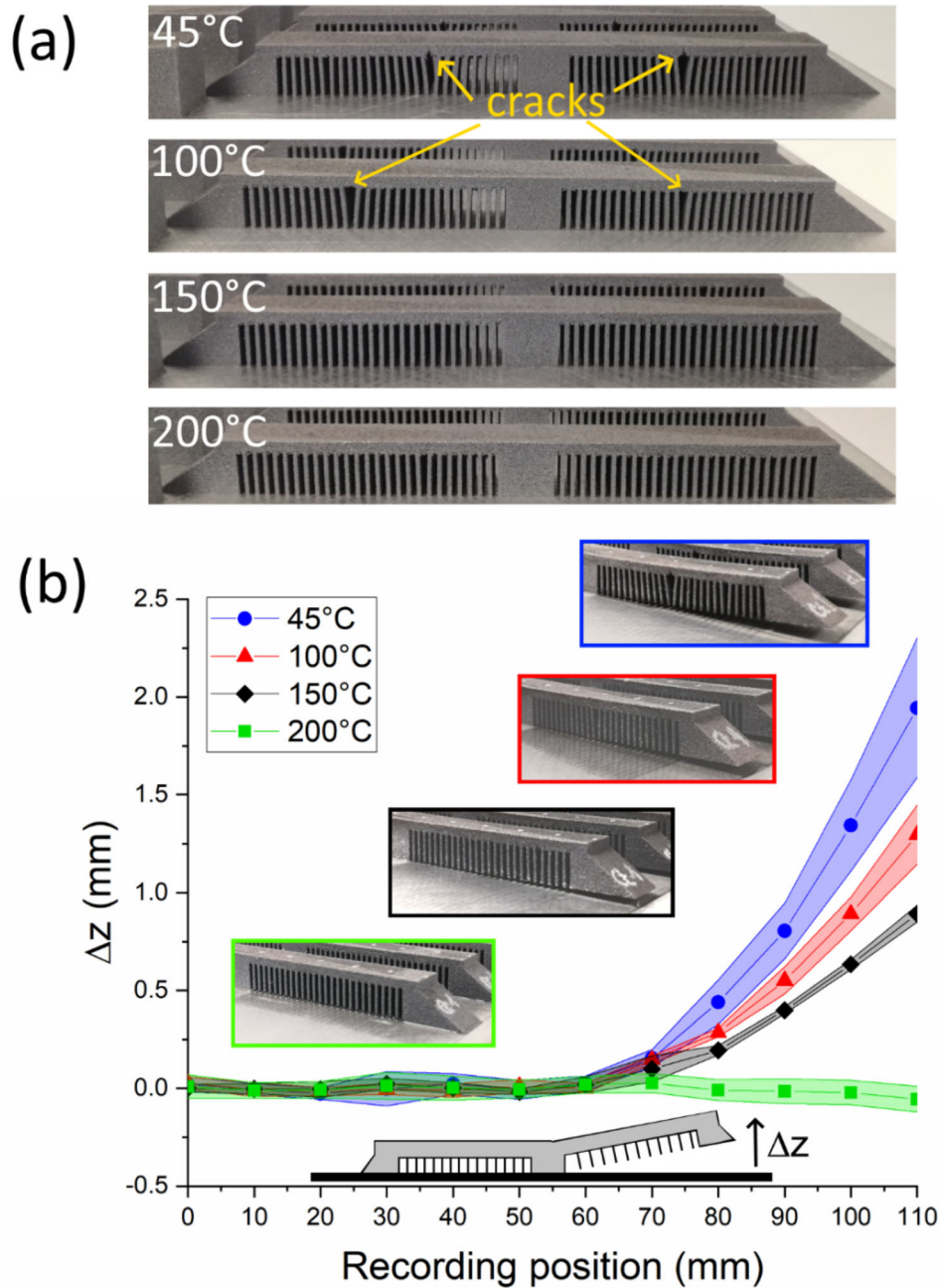
Fig. 4. (a) Macroscopic defects identified on twin cantilever samples at different platform heating temperatures; (b) deflection (ΔZ) of twin cantilever after removing from the supports at different platform heating temperatures. Colored bands represent the measured standard deviations along the length of one side of the cantilever (from center to end). Inset pictures show the distortions at different plate temperatures.

hardness profile after 53 h of printing time, a value drop in the curve can be identified. This suggests the occurrence of over-aging in this part of the sample. Specifically, a peak-age of around 138.6 HV is firstly encountered at τ of 13.4 h. Then, by further increasing τ, hardness is greatly reduced throughout the volume of material that experiences longer holding time, i.e., 49.2 h, on the heated platform. According to the results shown in Fig. 5, the AlSi10Mg building part has reached the peak-aged condition in most regions (up to $h = 27$ mm) using a

printing time of 13.4 h, whereas it is very probable that over-aging occurred when 53 h of LPBF printing time elapses.

Microstructural examination for selected positions of samples along the building direction further confirms the occurrence of in situ aging, as shown in Fig. 6. Based on these images, the overall response of AlSi10Mg alloy to the fast cooling rate of the LPBF process $(1 \times 10^5$ K/s)[19] results in a very fine microstructure with submicron-sized primary α-Al cells (gray color) surrounded by fibrous eutectic

boundaries (bright and light gray color). These eutectic boundaries are highly abundant in Si (see supplementary Fig. S-1), which is consistent with previous studies on SLM-produced AlSi10Mg.[20–22] Since the investigated alloy was known to be sensitive to precipitation hardening, the presence of various intracolumnar super-fine particles was remarkably higher when the samples experience longer holding times (Fig. 6e and f). There was no significant variation of α-Al column size in terms of dendrite width (λ = 0.39–0.44 μm). When the same sample height but different LPBF printing times were compared, a similar microstructural difference was found, i.e., the higher number density of precipitates in Fig. 6d–f than in Fig. 6a–c.

The hardness values of bulk AlSi10Mg samples processed with a platform temperature of 200°C and LPBF printing time of roughly 10 h are summarized in Fig. 7. As shown in the figure, two specific heat treatments have been designed. The former is a prolonged isothermal heat treatment at 200°C to extend the heated platform effect for longer printing times (up to 100 h). The latter is conventional T6-like heat treatment. Before the heat treatments, as-built samples show a hardness value of 100.5 ± 3 HV that is significantly far lower than those reported in the literature.[23,24] Hence, it seems that AlSi10Mg samples are already overaged after 10 h of printing time at 200°C. After isothermal heat treatment at 200°C for 100 h, a further decrease in hardness down to 91 ± 0.62 HV was revealed. However, by applying a T6-like heat treatment on both conditions, hardness values of 113.47 and 115.17 HV were obtained. These values correspond to a hardness increase of 12% and 26% for the as-built and isothermal heat-treated samples, respectively. Moreover, the hardness difference (roughly 10 HV) between the as-built and isothermal heat-treated samples is offset by applying the T6 heat treatment. All the measured HV values lie in a narrow range between 111 and 118 HV, which is very close to the previously reported peak-aged hardness of the alloy after T6 heat treatment.[25,26]

The general microstructure of the as-built sample after isothermal heat treatment at 200°C for 100 h is shown in Fig. 8a. The typical 'fish scale' pattern consists of dual-half elliptical melt pools aligned along the laser scanning direction. Figure 8b provides a representative high-magnification micrograph taken from the core region of a melt pool. Here, the microstructure mainly includes submicron-sized primary α-Al cells surrounded by fibrous eutectic architecture. The observed morphology of α-Al is, to some extent, columnar rather than cellular
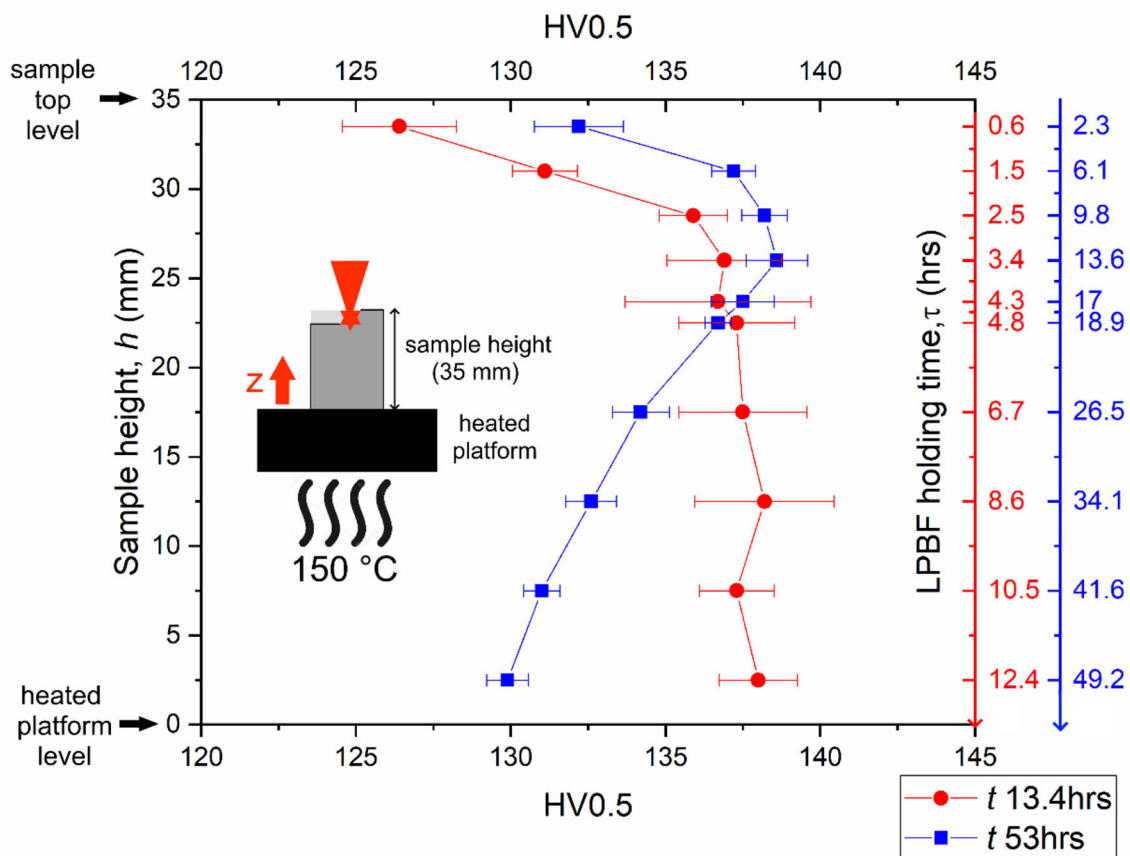

Fig. 5. Micro-hardness at different heights of AlSi10Mg samples built at different printing times (13.4 h and 53 h) at a platform temperature of 150°C. The hardness values are plotted as a function of the specimen heights and the corresponding LPBF holding times.
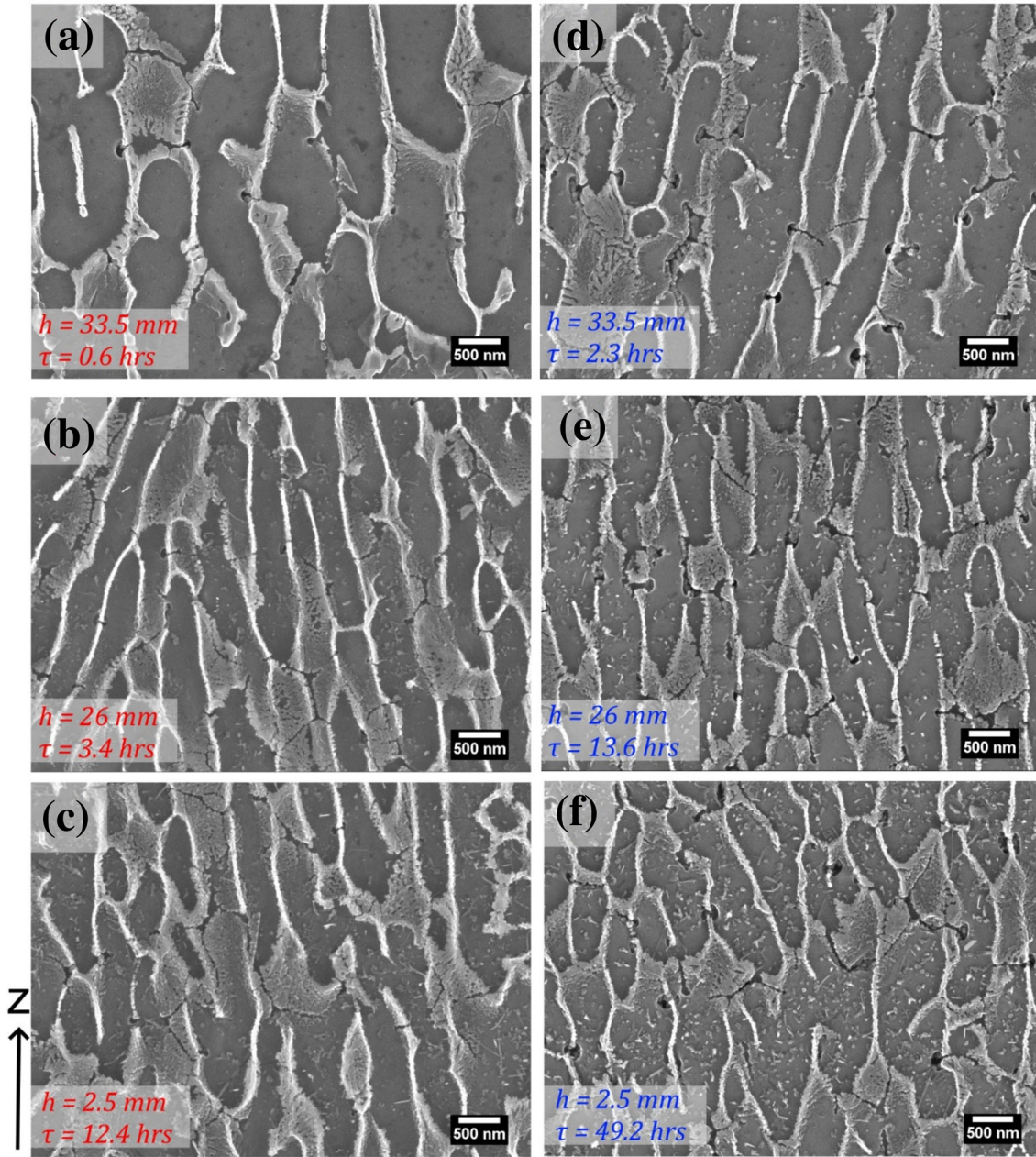
Fig. 6. Microstructure evolution along building direction of samples built upon (a–c) 13.4 h and (d–f) 53 h of printing time above a platform heated at 150°C. Micrographs in (a–c) and (d–f) are arranged according to decreasing sample height (h) or increasing LPBF holding time (τ) (from top to bottom) SEM investigations were performed in a melt pool core next to the corresponding HV measurements reported in Fig. 5.

because of the directional heat flux toward the building substrate. However, some rounded cells with a size of 0.41 ± 0.03 μm have also been identified. Moreover, a remarkable amount of tiny intracolumnar precipitates exist in the α-Al matrix. They most likely originate from the diffusion and precipitation of Si atoms.

Figure 8c and d provide representative micrographs of AlSi10Mg samples after isothermal heat treatment and subsequent T6-like heat treatment. In Fig. 8c, the 'fish-scale' microstructure almost

disappears because of the Al–Si eutectic and Si particles coarsening during the heat treatment. Note that few tracks of melt pool boundaries have been observed, as indicated by arrows in Fig. 8c. Inspection of the high-magnification image in Fig. 8d reveals the Si particles (see supplementary Fig. S-2) with a size range between 0.3 and 4 μm. Apart from these Si particles, elongated precipitates with a plate-like shape have also been observed. They have a maximum length of 12 μm and averaged thickness of 0.41 ± 0.12 μm. These
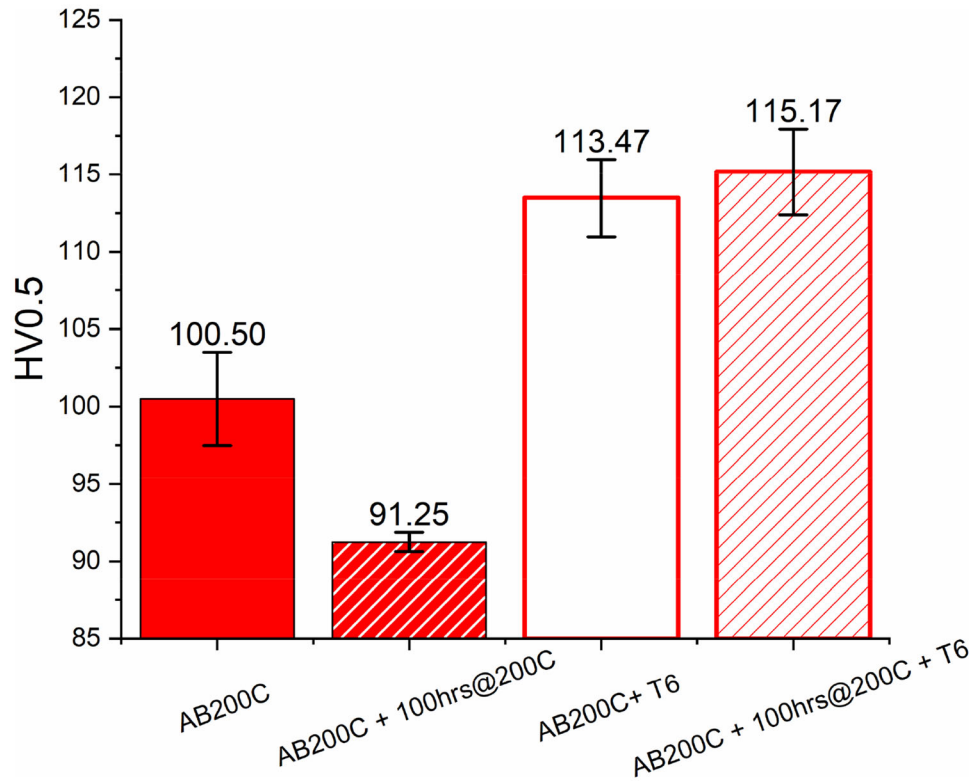
Fig. 7. Micro-hardness of the as-built and post-process heat-treated samples processed with a platform heating temperature of 200°C.

precipitates are the phase enriched in Fe, as evidenced by the EDS mapping shown in Fig. S-2. This type of precipitate was also reported previously in the SLM-produced A357 and AlSi10Mg after heat treatments.[9,20]

DISCUSSION

The production of massive AlSi10Mg parts involves essential challenges to deal with at the design stage due to the internal residual stresses formed from rapid cooling. As a result, preventing cracks and distortions has been the first key issue to be addressed. In this work, a building platform heating strategy was adopted throughout the printing process to alleviate internal residual stresses. Four heating temperatures were selected to find the proper temperature level to avoid cracks and distortions. The results revealed that these defects can be successfully prevented in cantilever samples produced at a platform temperature of 150°C and above. This can be explained by the fact that the solidification shrinkage of built parts can be reduced by the small temperature difference between the heated building platform and the AlSi10Mg solidus (557°C).[4,27] When the first powder layer of the cantilever arms is melted during LPBF, a natural thermal expansion of the melted alloy followed by a compression upon cooling is expected to occur. However, the shrinkage of the solidified layer is hindered by the robust support structure

underneath, creating high tensile residual stresses in the opposite direction, which in turn will lead to fins bending and then crack initiation.[15] By increasing the platform heating temperatures, the current results have shown that cantilever deflections decrease at 150°C and become negligible at 200°C. The findings are in good agreement with earlier research by Buchbinder et al.[15]

The Al-Si-Mg alloy is one of the main classes of heat-treatable alloys that exhibit apparent precipitation hardening response during aging.[28] Hence, it is technologically crucial to identify the in situ aging effect for long building time upon the heated platform because such an effect will eventually influence the mechanical properties of the parts. In this work, micro-hardness evaluation of parallelepiped samples processed on a platform heated up at 150°C with different printing times has shown distinct aging behavior (Fig. 5). For the printing time of 13.4 h, the measured hardness along the building direction was consistent with the results of a heat treatable SLM-produced A357 alloy reported by Casati et al.[29] It has to be noted that, in their work, a direct aging study was performed separately on bulk samples after the LPBF process, showing a peak-aged hardness of 137 HV for an aging time of 4 h at 160°C. In comparison, the same hardness value was achieved in the current work after around 3.4 h of holding time at a platform temperature of 150°C. As for the printing time of 53 h, our results
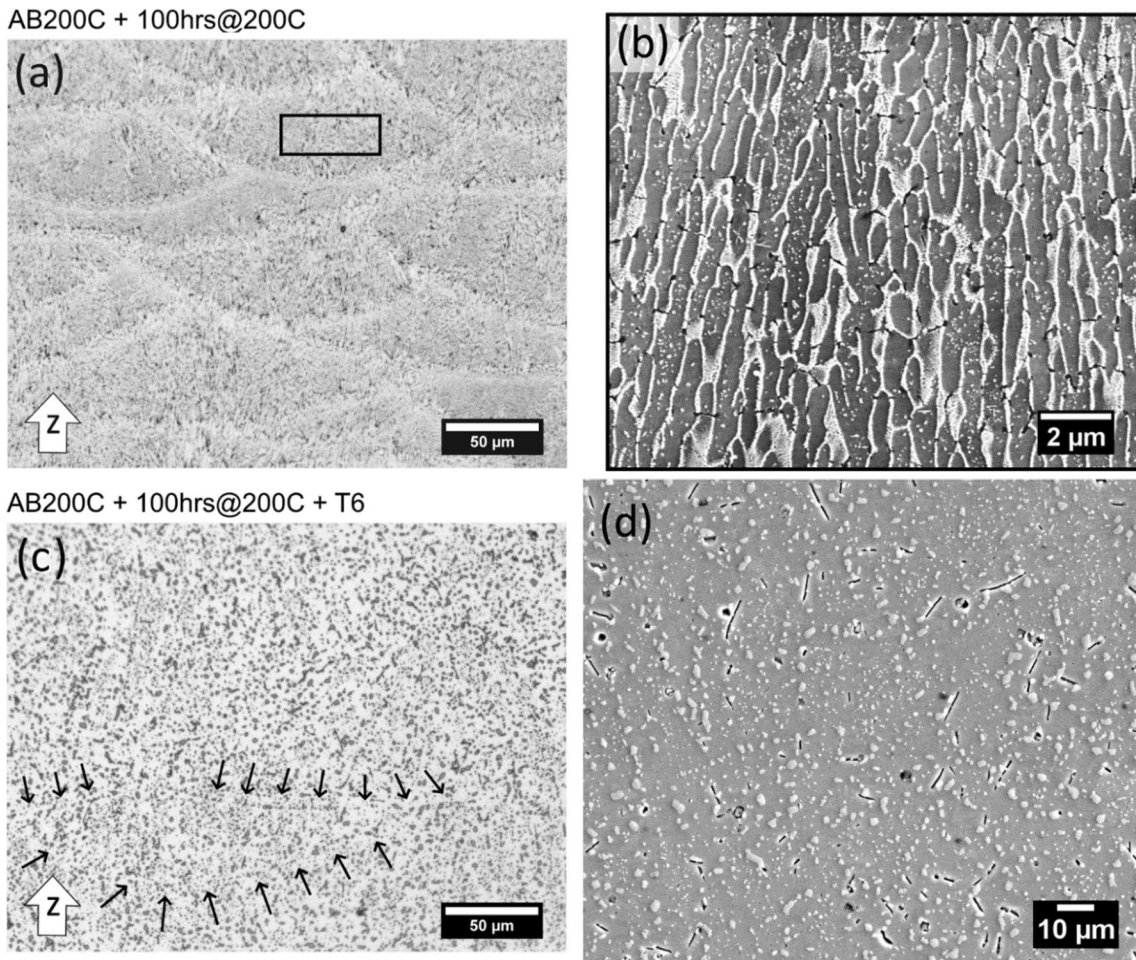
AB200C + 100hrs@200C

AB200C + 100hrs@200C + T6

Fig. 8. (a) Optical and (b) SEM micrographs of AlSi10Mg sample after isothermal heat treatment at 200°C for 100 h; (c) optical and (d) SEM micrographs of AlSi10Mg alloy after isothermal heat treatment (100 h at 200°C) plus T6-like heat treatment.

indicate the occurrence of over-aging throughout the sample. A similar aging response has been reported in previous work[13] for a SLM-produced AlSi10Mg alloy directly aged in a furnace at 160°C after printing on a non-heated platform. Also, the over-aging can be evidenced by the microstructure examination shown in Fig. 6f. The evolution of microstructure immediately after melting involves the consolidation of the Si-supersaturated α-Al liquid primarily into a cellular/columnar structure with an extended Si solute content. Later, the residual Si segregates at the cell boundaries, generating a fibrous eutectic texture.[21,30] Due to the intimate contact with the heated platform, it was also highly probable that the high holding time experienced at 150°C promotes the diffusion of the Si atoms in the α-Al supersaturated solid solution. In this way, massive precipitation of fine intracolumnar particles takes place accordingly, disrupting the eutectic network and affecting the hardness. These fine particles were previously identified as pure Si particles in a SLM-produced A357 alloy with direct aging at 160°C for 8 h.[9]

According to the current results, we advise adopting a platform temperature of 150°C and holding times lower than 13 h to prevent over-aging. Such a strategy will lead to more uniform hardness in the as-built sample and, simultaneously, partially release internal residual stresses without the need for post-process heat treatments. On the other hand, for large parts with critical shapes that require more than 13 h of LPBF printing, a platform temperature of 200°C can be used to reduce internal stresses. However, a relatively low hardness value will be obtained, which is coupled with a microstructure severely enriched by sub-micron particles (Fig. 8b). This weakening was ascribed to the former Si diffusion from the α-Al supersaturated solid solution that contributed to the formation of fine precipitates within Si cells and the concurrent low-temperature stress relieving, as recently reported in Refs. [31,32] by Fiocchi et al. In this case, a remedy to the over-aging phenomenon can be applied by using post-process heat treatment.[26,33,34] When the T6 heat treatment was applied, the current work witnessed a remarkable increase of hardness up to 115 HV, which is comparable to that

of die-cast A360-T6 counterparts.[25,35] Such strengthening is mainly due to the dispersion of Si spheroids, which can act as obstacles to dislocation motion.[34,36] It is interesting to note that most published works have reported a slight impoverishment of strength in the heat-treated condition,[9,25,34,36] which is different from the current results. The T6 heat treatment can also help to enhance fatigue properties of printed components, as documented by others.[8,37] Based on the above discussion, when LPBF processes large parts of aluminum, a new production strategy, including platform heating of 200°C and T6-like heat treatment, can be applied to achieve in situ stress relief and high hardness.

CONCLUSION

In summary, the present work set up a production strategy for LPBF to produce large parts of AlSi10Mg by considering two main aspects: the inevitable presence of residual stress that can cause job failure during a long printing time, and the in situ aging of the processed alloy. By using a platform heating strategy, we first defined the platform temperatures for preventing cracks and support distortions. Then, these temperatures were adopted in the second stage for the in situ aging investigations, leading to the following findings:

1. Building platform temperatures, set at 150°C and above, can effectively remove internal residual stresses and largely reduce part distortions for long-time LPBF jobs.
2. The in situ aging response occurs at a platform heating temperature of 150°C. The hardness reaches a peak with a holding time between 3.4 h and 13.4 h. Over-aging starts to appear when the holding time is longer than 13.4 h.
3. As-built and isothermal heat-treated samples processed at 200°C clearly show the over-aging response, reaching the lowest HV value after 100 h at 200°C.
4. A T6-like heat treatment was found to be able to recover the loss of hardness induced by over-aging at 200°C, increasing the HV value by 26% in the best scenario.

In conclusion, for producing large parts with critical shapes, a platform heating temperature of 200°C can be used to minimize distortions and bending of parts during LPBF. Nevertheless, the high printing time inevitably induces over-aging weakening, and the T6-like heat treatment can be applied to achieve mechanical properties comparable to the die-cast counterparts. On the other hand, for smaller parts requiring a printing time shorter than 13 h, a heated platform set at the aging temperature for Al alloys can be used to obtain directly peak-aged parts made of AlSi10Mg without the need for any post-process heat treatments.

CONFLICT OF INTEREST

The authors declare that they have no conflict of interest.

ELECTRONIC SUPPLEMENTARY MATERIAL

The online version of this article (https://doi.org/10.1007/s11837-020-04523-8) contains supplementary material, which is available to authorized users.

REFERENCES

1. D. Herzog, V. Seyda, E. Wycisk, and C. Emmelmann, *Acta Mater.* 117, 371 (2016).
2. N. Li, S. Huang, G. Zhang, R. Qin, W. Liu, H. Xiong, G. Shi, and J. Blackburn, *J. Mater. Sci. Technol.* 35, 242 (2018).
3. F. Calignano, *Mater. Des.* 64, 203 (2014).
4. P. Mercelis and J.P. Kruth, *Rapid Prototyp. J.* 12, 254 (2006).
5. M.F. Zaeh and G. Branner, *Prod. Eng.* 4, 35 (2010).
6. T. Kimura and T. Nakamoto, *Mater. Des.* 89, 1294 (2016).
7. H. Rao, S. Giet, K. Yang, X. Wu, and C.H.J. Davies, *Mater. Des.* 109, 334 (2016).
8. E. Brandl, U. Heckenberger, V. Holzinger, and D. Buchbinder, *Mater. Des.* 34, 159 (2012).
9. K.V. Yang, P. Rometsch, C.H.J. Davies, A. Huang, and X. Wu, *Mater. Des.* 154, 275 (2018).
10. U. Tradowsky, J. White, R.M. Ward, N. Read, W. Reimers, and M.M. Attallah, *Mater. Des.* 105, 212 (2016).
11. H.A. Ferguson, *Heat Treat. Alum. Alloys* 4, 841 (1991).
12. A. Aversa, M. Lorusso, F. Trevisan, E. Ambrosio, F. Calignano, D. Manfredi, S. Biamino, P. Fino, M. Lombardi, and M. Pavese, *Metals (Basel)* 7, 68 (2017).
13. M. Coduri, M. Hamidi Nasab, M. Vedani, R. Casati, and V. Tirelli, *Metals (Basel)* 8, 954 (2018).
14. J.H. Rao, Y. Zhang, K. Zhang, X. Wu, and A. Huang, *Mater. Des.* 182, 108005 (2019).
15. D. Buchbinder, W. Meiners, N. Pirch, K. Wissenbach, and J. Schrage, *J. Laser Appl.* 26, 012004 (2014).
16. F. Bosio, A. Aversa, M. Lorusso, S. Marola, D. Gianoglio, L. Battezzati, P. Fino, D. Manfredi, and M. Lombardi, *Mater. Des.* 181, 107949 (2019).
17. A.H. Maamoun, Y.F. Xue, M.A. Elbestawi, and S.C. Veldhuis, *Materials (Basel)* 12, 12 (2018).
18. A.H. Maamoun, Y.F. Xue, M.A. Elbestawi, and S.C. Veldhuis, *Materials (Basel)* 11, 2343 (2018).
19. T. DebRoy, H.L. Wei, J.S. Zuback, T. Mukherjee, J.W. Elmer, J.O. Milewski, A.M. Beese, A. Wilson-Heid, A. De, and W. Zhang, *Prog. Mater. Sci.* 92, 112 (2018).
20. L. Zhou, A. Mehta, E. Schulz, B. McWilliams, K. Cho, and Y. Sohn, *Mater. Charact.* 143, 5 (2018).

21. L. Thijs, K. Kempen, J.P. Kruth, and J. Van Humbeeck, *Acta Mater.* 61, 1809 (2013).
22. S. Marola, D. Manfredi, G. Fiore, M.G. Poletti, M. Lombardi, P. Fino, and L. Battezzati, *J. Alloys Compd.* 742, 271 (2018).
23. N.T. Aboulkhair, M. Simonelli, L. Parry, I. Ashcroft, C. Tuck, and R. Hague, *Prog. Mater Sci.* 106, 100578 (2019).
24. S. Marola, D. Gianoglio, F. Bosio, A. Aversa, M. Lorusso, D. Manfredi, M. Lombardi, and L. Battezzati, *J. Alloys Compd.* 821, 153538 (2020).
25. L. Girelli, M. Tocci, M. Gelfi, and A. Pola, *Mater. Sci. Eng. A* 739, 317 (2019).
26. A.H. Maamoun, M. Elbestawi, G.K. Dosbaeva, and S.C. Veldhuis, *Addit. Manuf.* 21, 234 (2018).
27. J.P. Kruth, J. Deckers, E. Yasa, and R. Wauthlé, *Proc. Inst. Mech. Eng. Part B J. Eng. Manuf.* 226, 980 (2012).
28. C.H.J. Davies, K. Zhang, J.H. Rao, X. Wu, A. Huang, and Y. Zhang, *Scr. Mater.* 160, 66 (2018).
29. R. Casati and M. Vedani, *Adv. Eng. Mater.* 1800406, 1800406 (2018).
30. K.G. Prashanth, S. Scudino, H.J. Klauss, K.B. Surreddi, L. Löber, Z. Wang, A.K. Chaubey, U. Kühn, and J. Eckert, *Mater. Sci. Eng. A* 590, 153 (2014).
31. J. Fiocchi, A. Tuissi, P. Bassani, and C.A. Biffi, *J. Alloys Compd.* 695, 3402 (2017).
32. J. Fiocchi and C.A. Biffi, *JOM* 72, 1118 (2020).
33. S. Li, J. Liu, Y. Shi, Q. Wei, W. Li, A. Zhang, C. Yan, and Y. Zhou, *Mater. Sci. Eng. A* 663, 116 (2016).
34. N.T. Aboulkhair, I. Maskery, C. Tuck, I. Ashcroft, and N.M. Everitt, *Mater. Sci. Eng. A* 667, 139 (2016).
35. L. Roger, *CSIRO Light Met. Flagsh.* (2008).
36. N.T. Aboulkhair, C. Tuck, I.A.N. Ashcroft, I.A.N. Maskery, and N.M. Everitt, *Metall. Mater. Trans. A* 46, 3337 (2015).
37. N.T. Aboulkhair, I. Maskery, C. Tuck, I. Ashcroft, and N.M. Everitt, *JMADE* 104, 174 (2016).